

Recoverable systems and the maximal hard-core model on the triangular lattice

GEYANG WANG ALEXANDER BARG
Univ. of Maryland, College Park, USA
{wanggy,abarg}@umd.edu

NAVIN KASHYAP
IISc, Bangalore, India
nkashyap@iisc.ac.in

Abstract—In a previous paper (arXiv:2510.19746), we have studied the maximal hard-core model on the square lattice \mathbb{Z}^2 from the perspective of recoverable systems. Here we extend this study to the case of the triangular lattice \mathbb{A} . The following results are obtained: (1) We derive bounds on the capacity of the associated recoverable system on \mathbb{A} ; (2) We show non-uniqueness of Gibbs measures in the high-activity regime; (3) We characterize extremal periodic Gibbs measures for sufficiently low values of activity.

1. INTRODUCTION: THE MAXIMAL HARD-CORE MODEL

We consider assignments of bits to the sites (vertices) of a lattice $\mathcal{L} \subset \mathbb{R}^2$, called configurations. A recovery condition is a function that determines the value of a site, i , from the values of its neighbors in \mathcal{L} , and a collection of all configurations that follow a particular recovery condition is called a recoverable system. Motivated by the concept of codes with local reconstruction [1], one-dimensional recoverable systems were introduced in [2] both in the deterministic and probabilistic settings. In [3], we argued that 2D systems can be adequately viewed as interaction models of statistical mechanics. A detailed study of recoverable systems on the square lattice, \mathbb{Z}^2 , using tools from statistical mechanics was conducted in [4]. In that work, we observed that recoverable systems on \mathbb{Z}^2 under a particular recovery condition considered there can be viewed as instances of the *maximal hard-core model* on \mathbb{Z}^2 . The hard-core model without the maximality restriction has been extensively studied in the literature, see e.g., [5], [6], [7]. Establishing this connection provides a set of tools that enables the analysis of the maximal case.

In this work, we extend this study to the case of the triangular lattice \mathbb{A} , a.k.a. the hard-hexagon model [8]. The hard-core model on \mathbb{A} was recently studied in [9], and extending it to the maximal case forms a natural mathematical problem. It is also motivated by applications in storage systems: while the square lattice has been frequently used as a model of storage devices, the triangular lattice has also been proposed for modeling the layout of glass-ceramic HDD platters and magnetic bit-patterned media [10], [11].

Below we denote a recoverable system on \mathcal{L} by $\mathcal{X}(\mathcal{L})$, omitting the mention of the lattice when it is clear or not important. We aim to derive capacity bounds for the system \mathcal{X} and to initiate a study of the Gibbs measures, governed by an activity parameter λ that can be defined on it.

Gibbs measures for the hard-core model are traditionally studied in statistical mechanics (see e.g. [12], [13]). Our added

motivation for their study is information-theoretic: We would like to define measures on the recoverable system \mathcal{X} with a view to understanding its ability to convey information reliably across a noisy channel. In particular, our interest is in determining, for a given noisy channel, the mutual information rate between channel input and output, when the input to the channel is a configuration drawn from a suitably defined measure μ on \mathcal{X} . The idea then would be to maximize the mutual information rate over measures μ belonging to some parameterized class, such as the Gibbs measures we study in this paper. While the execution of this project is beyond the scope of this paper, we note that it fits into a long line of work on the capacity of channels with constrained inputs [14]–[20].

1.1 Definitions

Given a configuration $\omega \in \{0, 1\}^{\mathcal{L}}$, we consider the following recovery condition: for any site $i \in \mathcal{L}$, the value $\omega_i = 1$ if and only if $\omega_j = 0$ for all $j \sim i$, i.e., all the sites j adjacent to i in the graph of \mathcal{L} . It is easy to see that for any $\omega \in \mathcal{X}$, the support $\text{supp}(\omega)$ forms a maximal independent set (MIS) in \mathcal{L} . Examples of maximal independent sets in (finite regions in) \mathbb{Z}^2 and \mathbb{A} are shown in Fig. 1. Introducing the *activity parameter* λ , we can construct a family of Gibbs measures on \mathcal{X} as defined below. By analogy with the well-known hard-core model of statistical physics [7], [8], [21], we call the obtained random field the *maximal hard-core model*. While it has previously appeared in physics literature, e.g., [22], this work and the previous paper [4] appear to be the first to consider its mathematical aspects.

For a configuration $\omega \in \mathcal{X}(\mathcal{L})$ we denote by ω_Λ its restriction to a finite region $\Lambda \Subset \mathcal{L}$. Denote the complement of Λ in \mathcal{L} by Λ^c and let $\omega_{\Lambda^c} := (\omega_i)_{i \in \Lambda^c}$, $|\omega_\Lambda| := |\text{supp}(\omega_\Lambda)|$.

Definition 1.1 (The maximal hard-core model). A probability measure μ on $\mathcal{X}(\mathcal{L})$ is called a *maximal hard-core Gibbs measure* with activity $\lambda > 0$ if, for every finite set $\Lambda \Subset \mathcal{L}$, $\eta \in \mathcal{X}(\mathcal{L})$ and μ -almost every $\omega \in \mathcal{X}(\mathcal{L})$, the conditional probability on Λ satisfies

$$\mu_\Lambda(\eta \mid \omega) = \begin{cases} \frac{\lambda^{|\eta_\Lambda|}}{\mathcal{Z}_{\Lambda, \lambda}^\omega} & \text{if } \eta_{\Lambda^c} = \omega_{\Lambda^c}, \\ 0 & \text{otherwise,} \end{cases} \quad (1)$$

where the partition function is given by

$$\mathcal{Z}_{\Lambda, \lambda}^\omega = \sum_{\eta \in \mathcal{X}(\mathcal{L}) : \eta_{\Lambda^c} = \omega_{\Lambda^c}} \lambda^{|\eta_\Lambda|}.$$

We note that maximum hard-core measures always exist; a formal argument for \mathbb{Z}^2 is presented in [4, App.C].

The main contributions of this paper are the following:

- (1) We derive bounds on the capacity of the recoverable system on $\mathcal{X}(\mathbb{A})$ defined above;
- (2) We show that for large λ there exist at least two Gibbs measures on $\mathcal{X}(\mathbb{A})$ (phase coexistence in the high-activity regime);
- (3) We characterize extremal periodic Gibbs measures for sufficiently low values of activity.

Previously, similar results for the case of $\mathcal{L} = \mathbb{Z}^2$ were obtained in [4].

2. CAPACITY OF THE SYSTEM

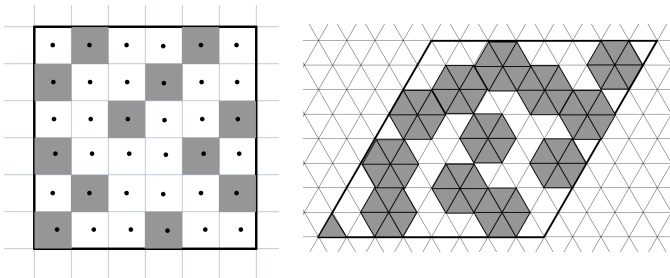
Capacity or topological entropy of the system $\mathcal{X}(\mathbb{A})$ is defined through a limiting procedure. We assume that all edges in \mathbb{A} have length 1. We will always label sites in \mathbb{A} by their coordinates in the basis $(\mathbf{b}_1, \mathbf{b}_2) = ((1, 0), (\frac{1}{2}, \frac{\sqrt{3}}{2}))$. A configuration η in a finite region $\Lambda \Subset \mathbb{A}$ is called *compatible* if there exists $\omega \in \mathcal{X}(\mathbb{A})$ such that $\eta = \omega_\Lambda$, and it is called *maximal* if every 0 is adjacent to at least one 1 and it does not contain adjacent 1's. Equivalently, the support of a maximal configuration η is a MIS in the subgraph induced by Λ . Let $\Lambda_{n,m} = \{1, \dots, n\} \times \{1, \dots, m\}$ and $\Lambda_n = \Lambda_{n,n}$. The topological entropy of $\mathcal{X}(\mathbb{A})$ is defined as

$$H_0 := \lim_{n \rightarrow \infty} \frac{\log_2 |\mathcal{X}_{\Lambda_n}(\mathbb{A})|}{|\Lambda_n|}, \quad (2)$$

where $\mathcal{X}_{\Lambda_n}(\mathbb{A})$ is the collection of compatible configurations on Λ_n , and $|\Lambda_n|$ denotes the number of sites in Λ_n . The limit in Eq. (2) exists due to subadditivity.

2.1 Relation to subshifts of finite type

The fact that the system $\mathcal{X}(\mathbb{A})$ has positive capacity follows from its description as a subshift of finite type (SFT), i.e., a collection of configurations $\mathcal{X} \subset \{0, 1\}^{\mathcal{L}}$ defined by forbidding finitely many local patterns.



(a) Each square is centered on a site in \mathbb{Z}^2 . Occupied sites are shown by filled squares.

(b) Occupied sites are shown as centers of filled hexagons. A set of centers forms a MIS if and only if there is no room to fit another filled hexagon.

Fig. 1: Maximal independent sets in \mathbb{Z}^2 and \mathbb{A} .

It is easy to see that $\mathcal{X}(\mathbb{A})$ is equivalent to an SFT defined by forbidding the following patterns:

$$\begin{array}{ccccccc} & & & & 0 & 0 & \\ & & & & 0 & 0 & 0 \\ 1 & 1 & & & & & \\ & & 1 & & & & \\ & & & 1 & & & \\ & & & & 0 & 0 & \\ & & & & 0 & 0 & \end{array}$$

An SFT is called *strongly irreducible* if there exists an $r > 0$ such that for all finite regions $A, B \in \mathcal{L}$ with ℓ_1 distance $\geq r$, for every pair of configurations $\omega, \eta \in \mathcal{X}$, there exists $\sigma \in \mathcal{X}$ such that $\sigma_A = \omega_A$ and $\sigma_B = \omega_B$. As shown in [23], a strongly irreducible SFT on a 2D lattice with at least 2 elements has positive topological entropy.

Lemma 2.1. *A maximal configuration η on $\Lambda_{n,m}$, $n, m \geq 1$ is compatible.*

Proof: Consider the enlarged rectangle, $\Lambda_{n+1,m+1}$. The support of η forms an independent set in it, which can be extended to a MIS in $\Lambda_{n+1,m+1}$. By induction, we conclude that there exists an $\omega \in \mathcal{X}(\mathbb{A})$ such that $\omega_{\Lambda_{n,m}} = \eta$. ■

Proposition 2.2. (a) *The recoverable system $\mathcal{X}(\mathbb{A})$ is a strongly irreducible SFT with $r = 4$.*

(b) *Let σ and η be maximal configurations in $\Lambda_{n,m}$ and $(m+1, 0) + \Lambda_{n,m}$, respectively. There exists a maximal compatible configuration ω on $\Lambda_{n,2m+1}$ such that $\omega_{\Lambda_{n,m}} = \sigma$ and $\omega_{(m+1,0)+\Lambda_{n,m}} = \eta$.*

Proof: Strong irreducibility can be proved by noticing that the argument in Prop. A.2 in [4], written there for the \mathbb{Z}^2 lattice, is in fact independent of this assumption. The procedure of constructing σ described in the proof applies to the triangular lattice equally well.

To prove (b), let $\bar{\omega}$ be a configuration on $\Lambda_{n,2m+1}$ such that $\bar{\omega}_{\Lambda_{n,m}} = \sigma$, $\bar{\omega}_{(m+1,0)+\Lambda_{n,m}} = \eta$ and $\bar{\omega}_i = 0$ for all $i \in (\Lambda_{n,m} \cup (m+1, 0) + \Lambda_{n,m})^c$. The configuration $\bar{\omega}$ corresponds to an independent set in $\Lambda_{n,2m+1}$, which must be contained in a MIS in $\Lambda_{n,2m+1}$. Let ω be such that its support forms this MIS. Observe that $\bar{\omega}_i = \omega_i$ for all $i \in \Lambda_{n,m+1}$ except possible the sites $i \in \{1, \dots, n\} \times \{m+1\}$. By Theorem 2.1, ω is compatible. ■

A shift-invariant maximal hard-core Gibbs measure with $\lambda = 1$ maximizes the measure-theoretic entropy, which we proceed to define. Let P be a *shift-invariant* probability measure on $\mathcal{X}(\mathbb{A})$, the *entropy rate* of P is defined by

$$H(P) = \lim_{n \rightarrow \infty} -\frac{1}{|\Lambda_n|} \sum_{\eta \in \mathcal{X}_{\Lambda_n}(\mathbb{A})} P(\Pi_{\Lambda_n}^{-1}(\eta)) \log_2 P(\Pi_{\Lambda_n}^{-1}(\eta))$$

where $\Pi_{\Lambda_n} : \mathcal{X}(\mathbb{A}) \mapsto \mathcal{X}_{\Lambda_n}(\mathbb{A})$ is the projection map $\Pi_{\Lambda_n}(\omega) := \omega_{\Lambda_n}$, and $\Pi_{\Lambda_n}^{-1}(\eta) = \{\omega \in \mathcal{X}(\mathbb{A}) : \omega_{\Lambda_n} = \eta\}$ is a cylinder set.

The variational principle implies that $H_0 = \sup_P H(P)$, where the supremum is taken over all shift-invariant probability measures P on $\mathcal{X}(\mathbb{A})$ [24, Sec. 4.5]. Moreover, the supremum is achieved if and only if P has *uniform conditional probabilities*. That is, given $\omega \in \mathcal{X}(\mathbb{A})$, for every finite region $\Lambda \Subset \mathbb{A}$, $P_\Lambda(\cdot | \omega)$ is a uniform distribution on $\{\eta \in \mathcal{X}(\mathbb{A}) : \eta_{\Lambda^c} = \omega_{\Lambda^c}\}$ (see [25, Proposition 1.8]).

Proposition 2.3. *Let μ be a shift-invariant maximal hard-core Gibbs measure with $\lambda = 1$. Then $H(\mu) = H_0$.*

Proof: The proof is immediate by (1), since $\mu_\Lambda(\cdot | \omega)$ is a uniform distribution when $\lambda = 1$. ■

Observe that a shift-invariant maximal hard-core Gibbs measure can be prepared with a periodic boundary condition.

2.2 Capacity and encoding schemes

In [4] we showed that the capacity of $\mathcal{X}(\mathbb{Z}^2)$ satisfies $0.3012 \leq H_0 \leq 0.3409$ relying on a standard transfer matrix computation for the 2-dimensional SFT; see, e.g., [26]. Here we establish analogous bounds for $\mathcal{X}(\mathbb{A})$

Proposition 2.4. *The topological entropy of $\mathcal{X}(\mathbb{A})$ satisfies $0.4609 \leq H_0 \leq 0.4807$.*

Proof sketch: Denote by $\mathcal{M}_{\Lambda_{n,m}}(\mathbb{A})$ be the collection of maximal configurations on $\Lambda_{n,m}$. We use configurations in $\mathcal{M}_{\Lambda_{n,m}}(\mathbb{A})$ to construct configurations in $\mathcal{X}(\mathbb{A})$ as follows. Partition \mathbb{A} into disjoint blocks of size $(m+1) \times (n+1)$ with the form $(t_1(m+1), t_2(n+1)) + \Lambda_{n+1, m+1}$, where $t_1, t_2 \in \mathbb{Z}$. For each block, we place an arbitrary configuration from $\mathcal{M}_{\Lambda_{n,m}}(\mathbb{A})$ into the top-left corner of the block. The bottom and right edges of each block can be filled according to Proposition 2.2 part (ii). Therefore, $|\mathcal{X}_{\Lambda_{n+1, m+1}}(\mathbb{A})| \geq |\mathcal{M}_{\Lambda_{n,m}}(\mathbb{A})|$ and

$$H_0 = \lim_{m, n \rightarrow \infty} \frac{\log_2 |\mathcal{X}_{\Lambda_{n+1, m+1}}(\mathbb{A})|}{(m+1)(n+1)} \geq \frac{\log_2 |\mathcal{M}_{\Lambda_{n,m}}(\mathbb{A})|}{(m+1)(n+1)}. \quad (3)$$

The number $|\mathcal{M}_{\Lambda_{n,m}}(\mathbb{A})|$ of MISs on $\Lambda_{n,m}$ which can be computed by an application of the transfer matrix method as discussed in [4, App. D.1]. To obtain the lower bound in the claim, we take $n = 10$ and $m = 132$ and perform the calculation.

On the other hand, the number of independent sets $I(n)$ in the graph $\Lambda_n \in \mathbb{A}$ satisfies $\lim_{n \rightarrow \infty} I(n)^{1/n^2} = k_h$, where $k_h := 1.39548\dots$ is given by [8]. Therefore, $|\mathcal{X}_{\Lambda_n}(\mathbb{A})| \leq I(n)$ and we have that

$$\begin{aligned} H_0 &= \lim_{n \rightarrow \infty} \frac{\log_2 |\mathcal{X}_{\Lambda_n}(\mathbb{A})|}{n^2} \\ &\leq \lim_{n \rightarrow \infty} \frac{\log_2 I(n)}{n^2} = \log_2 k_h \leq 0.4807. \end{aligned} \quad (4)$$

Encoding procedure: The problem of encoding a constrained system has often been considered in information theory literature based on Markov conditions or tiling considerations [27], [28]. We confine ourselves to the following simple remark. Let $N := \lfloor \log_2 |\mathcal{M}_{n,m}(\mathbb{A})| \rfloor$. To encode an infinite bit string x into a configuration $\omega \in \mathcal{X}(\mathbb{A})$, we begin with establishing an arbitrary bijection ϕ between segments $s_t = \{tN, \dots, (t+1)N\}$, $t \in \mathbb{Z}$ and pairs of integers $(t_1, t_2) \in \mathbb{Z}^2$. Let $f : \{0, 1\}^N \mapsto \mathcal{M}_{n,m}(\mathbb{A})$ be a function that encodes an N -bit string into a MIS on $\Lambda_{n,m}$. For each $t \in \mathbb{Z}$, we place $f(x_{s_t})$ in the top-left corner of the block $(t_1(m+1), t_2(n+1)) + \Lambda_{n+1, m+1}$, where t and (t_1, t_2) are related through ϕ . The unfilled lines between the $n \times m$ blocks can be filled by a recursive application of Theorem 2.2 (b). As $n, m \rightarrow \infty$, this encoder achieves at least the “rate” 0.4609. ■

3. PHASE COEXISTENCE: THE HIGH-ACTIVITY REGIME

The general approach to establishing a lower bound on λ for phase coexistence relies on identifying a “distinguishing event” that has markedly different probabilities of occurrence under some pair of distinct boundary conditions. This idea

goes back to Dobrushin’s foundational work [29], and it has been widely adopted in the mathematical literature. A development of this idea enables us to prove the following theorem, which forms the main result of this section.

Theorem 3.1. *The maximal hard-core model on \mathbb{A} exhibits a phase coexistence for sufficiently large λ .*

We will show that this statement holds true for all $\lambda > 15^6$. We believe that this bound can be improved based on more accurate contour counting in the lattice. An analogous result for \mathbb{Z}^2 , established in [4], holds for all $\lambda > 6.35$ and relies on earlier results of [7] on counting special-type walks in \mathbb{Z}^2 (the “taxi-walk connective constant”).

The triangular lattice can be naturally partitioned into 3 sublattices, one of which is spanned by the vectors $(0, \sqrt{3})$, $(\frac{3}{2}, \frac{\sqrt{3}}{2})$ and the other two are its shifts. This partition defines a 3-coloring of the vertices of \mathbb{A} shown in Fig 3.

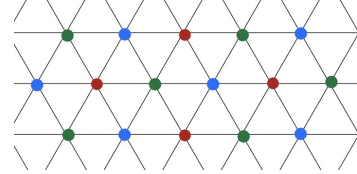


Fig. 3: A coloring of the vertices of \mathbb{A}

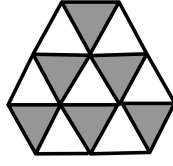
Let ω^r , ω^g , and ω^b be the configurations supported on all red, green, and blue vertices, respectively. Recall that $\Lambda_n = \{1, \dots, n\} \times \{1, \dots, n\} \subset \mathbb{A}$ is a rhombus and $\Lambda_n^c = \mathbb{A} \setminus \Lambda_n$ is its complement. Consider the set of configurations $\omega \in \mathcal{X}(\mathbb{A})$ such that all the vertices of some fixed color, say blue, in Λ_n^c are occupied; see Fig. 4a below. We say that these ω ’s follow the blue *boundary condition*. Denote by \mathcal{J}_n^b the set of all configurations contained in $\mathcal{X}(\mathbb{A})$ that agree with ω^b outside Λ_n . The corresponding Gibbs distribution on Λ_n is given by

$$\mu_n^b(\eta) := \mu_{\Lambda_n}(\eta \mid \omega^b) = \frac{\lambda^{|\eta_{\Lambda_n}|}}{\mathcal{Z}_n^b},$$

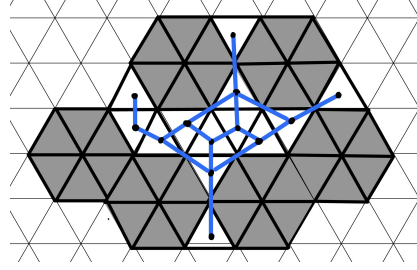
where $\eta \in \mathcal{J}_n^b$ and $\mathcal{Z}_n^b = \sum_{\eta \in \mathcal{J}_n^b} \lambda^{|\eta_{\Lambda_n}|}$. The measure μ_n^b is supported on \mathcal{J}_n^b . The Gibbs distributions μ_n^r, μ_n^g under the red and green boundary conditions are defined analogously. The Gibbs measures obtained as weak subsequential limits of $\{\mu_n^b\}_n, \{\mu_n^r\}_n, \{\mu_n^g\}_n$ for $n \rightarrow \infty$ are denoted by μ^b, μ^r, μ^g respectively.

Let $\omega \in \mathcal{X}(\mathbb{A})$ be a maximal independent set in \mathbb{A} . Below we call triangles in the lattice *faces*. A face is *empty* if it is not incident to any of the occupied vertices in ω . Two faces are called *adjacent* if they share a vertex and are called *connected* if they either share an edge (called *edge-connected*) or they share a single vertex and are not both adjacent to a common face (called *point-connected*); see Fig. 2a. A configuration, ω , gives rise to a maximal packing of hexagons, which inherit their colors from the center (occupied) sites. A face contained in a blue hexagon will itself be called blue, and similarly for the other colors. Empty faces are uncolored.

Faces of \mathbb{A} span a 6-regular graph, $G_{\mathbb{A}}$, where two faces are connected if they are connected in the sense of the above definition. A (simple) path in $G_{\mathbb{A}}$ is a sequence of connected



(a) The central face is adjacent to 12 faces and connected to 6 of them, filled in gray.



(b) Filled hexagons are centered on occupied vertices in ω . An empty face can have between 2 and 4 empty neighbors. This defines a subgraph associated with the contour, used in the counting argument in Theorem 3.4.

Fig. 2: Connectivity and contours

vertices in which no vertex appears twice. A path is called edge-connected if the vertices in the sequence are edge-connected. The restriction of $G_{\mathbb{A}}$ to Λ_n will be denoted G_{Λ_n} ; see Fig. 2.

Definition 3.1. Given a configuration $\omega \in \mathcal{X}(\mathbb{A})$ subject to a boundary condition, a *contour*, γ , is a maximal connected component in Λ_n formed by empty faces. The set of faces in \mathbb{A} (vertices of $G_{\mathbb{A}}$) from which there is an edge-connected path to infinity not intersecting γ is called the exterior of the contour, denoted γ_{\circ} ; see Fig. 4a. The contour interior is defined as $\gamma_{\bullet} := \mathbb{A} \setminus (\gamma \cup \gamma_{\circ})$.

For instance, in Fig. 4a the exterior γ_{\circ} is formed of all the blue faces, extending to infinity in all directions, and γ_{\bullet} is the green hexagons and the region that they encompass.

Similar “thick” contours were previously considered in [30]. The collection of contours defined by ω is denoted by $\Gamma(\omega)$, and $\Gamma := \cup_{\omega \in \mathcal{X}(\mathbb{A})} \Gamma(\omega)$. Properties of the contours are given in the next lemma.

Lemma 3.2. *Let ω_{Λ_n} be a configuration and $\gamma \in \Gamma(\omega)$ be a contour associated with it.*

(a) *The exterior γ_{\circ} forms a unique infinite connected component.*

(b) *A face in the contour has between 2 and 4 neighbors (Fig. 2b).*

(c) *γ encloses a finite domain inside Λ_n , which may contain other contours.*

(d) *The faces of γ_{\circ} connected to γ have the same color.*

Proof: Part (a) follows by definition. For the other parts of the proof, we note that the only way to prevent a contour from extending in a particular direction is to have a group of edge-connected hexagons blocking that direction, and that such hexagons necessarily have the same color. Turning to Part (b), we note that an empty face can have degree one if it is edge- or vertex-connected to a single face. In either case, it is not possible to place same-color hexagons to block all other connections. Examples of degrees 3 and 4 are given in Fig. 2b. Finally, if 5 out of the 6 faces connected to an empty face e are themselves empty, then either 3 of them are node-connected to e , or 3 are edge-connected to it. In either case, this forces an empty hexagon as illustrated in Fig. 5.

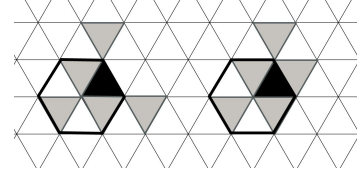


Fig. 5: Two possible cases with an empty triangle (filled in black), five of whose neighbor triangles (filled in gray) are also empty. Each of these arrangements forces an empty hexagon, so they cannot arise in a MIS. This shows that the degree of the graph associated with a contour is at most 4.

Let us prove Part (c). We have assumed that Λ_n satisfies some (say, blue) boundary condition. It is possible that some of the hexagons inside Λ_n , edge-connected to the blue exterior of Λ_n , are blue, such as in the upper corner in Fig. 4. Accounting for all such hexagons, this creates a new boundary that encloses a finite domain. The hexagons closest to this boundary are vertex-connected to it or one edge away from it; they are necessarily red or green; therefore, all the faces edge-connected to the boundary will be empty, and thus, a part of the contour. This part contains a simple cycle, which can be formed of the faces identified above. This cycle encloses a finite domain which includes the interior, γ_{\bullet} . This argument also covers the case of other contours which may be contained inside the contour adjacent to the boundary, such as the one in Fig. 4a.

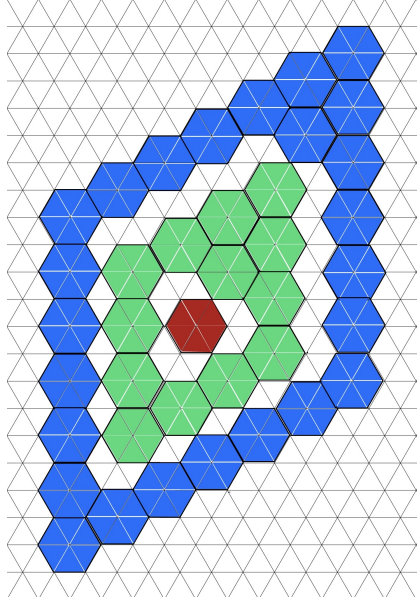
This argument also proves part (d). Indeed, faces of γ_{\circ} connected to γ are necessarily edge-connected. As discussed above, these faces are blue, as claimed. ■

Below we say that γ is a red (blue, green) contour, if the color identified in Theorem 3.2(d) is red (blue, green, respectively).

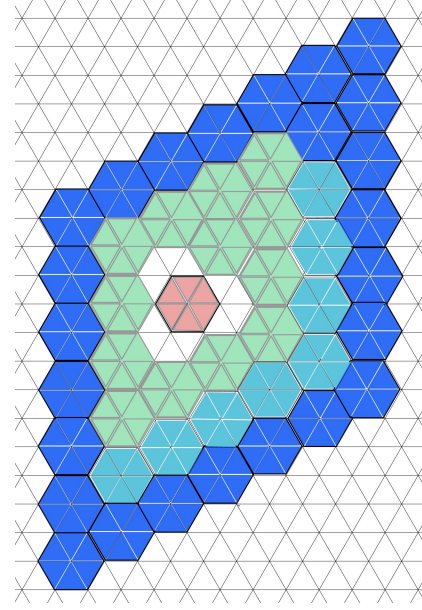
For a fixed number $m < n$, define $\Lambda_m^E = \{-m, \dots, m + 1\} \times \{-m, m\}$ ($\Lambda_m^W = \{-m - 1, \dots, m\} \times \{-m, \dots, m\}$) be the collection of vertices that are contained in Λ_m and the right (left) neighbors of Λ_m .

Given a configuration $\eta \in \mathcal{X}(\mathbb{A})$, we say that

- η is m -red if all red vertices in Λ_m^E are occupied.
- η is m -green if all green vertices in Λ_m^W are occupied.
- η is m -homogeneous if it is either m -green or m -red.



(a) A maximal independent set satisfying the blue boundary condition, giving rise to two contours shown by empty triangles inside the rhombus, Λ_n .



(b) The configuration in Fig. 4a upon applying the shift, ϕ . The green island shifted NW, becoming blue. The shift includes the inner contour and its interior.

Fig. 4: Illustrating the contour erasing procedure.

To prove Theorem 3.1, we seek to construct an event for which the conditional probabilities differ under the two limiting measures. Specifically, let \mathcal{R}_m denote the event that a configuration is m -red, and \mathcal{G}_m the event that it is m -green. We will show that for all $n > m$ and sufficiently large m ,

$$\mu_n^r(\mathcal{G}_m \mid \mathcal{G}_m \cup \mathcal{R}_m) \leq \frac{1}{3}, \quad (5)$$

and

$$\mu_n^g(\mathcal{G}_m \mid \mathcal{G}_m \cup \mathcal{R}_m) \geq \frac{2}{3}. \quad (6)$$

These inequalities show that, under the condition that a configuration is m -homogeneous, the red boundary condition ω^r implies that it is unlikely to be m -green, and vice versa. Since the limiting Gibbs measures depend on the boundary condition, Eqs. (5) and (6) together imply the claimed phase coexistence.

Let $\mathcal{B}_{m,n}^r$ ($\mathcal{A}_{m,n}^r$) be the set of m -green (resp., m -homogeneous) configurations that are consistent with the red boundary condition ω^r outside Λ_n . To prove (5), we will construct a mapping $\phi : \mathcal{B}_{m,n}^r \mapsto \mathcal{A}_{m,n}^r \setminus \mathcal{B}_{m,n}^r$ such that for a fixed large m and $\tau \in \mathcal{A}_{m,n}^r \setminus \mathcal{B}_{m,n}^r$,

$$\sum_{\substack{\eta \in \mathcal{B}_{m,n}^r \\ \phi(\eta) = \tau}} \lambda^{|\eta_{\Lambda_n}| - |\tau_{\Lambda_n}|} \leq \frac{1}{3} \quad (7)$$

holds for all $\eta \in \mathcal{B}_{m,n}^r$. Once (7) is proved, we find

$$\mu_n^r(\mathcal{G}_m \mid \mathcal{G}_m \cup \mathcal{R}_m) = \frac{\sum_{\eta \in \mathcal{B}_{m,n}^r} \lambda^{|\eta_{\Lambda_n}|}}{\sum_{\eta \in \mathcal{A}_{m,n}^r} \lambda^{|\eta_{\Lambda_n}|}}$$

$$\begin{aligned} &= \frac{\sum_{\eta \in \mathcal{B}_{m,n}^r} \lambda^{|\phi(\eta)_{\Lambda_n}|} \cdot \lambda^{|\eta_{\Lambda_n}| - |\phi(\eta)_{\Lambda_n}|}}{\sum_{\eta \in \mathcal{A}_{m,n}^r} \lambda^{|\eta_{\Lambda_n}|}} \\ &= \frac{\sum_{\tau \in \mathcal{A}_{m,n}^r \setminus \mathcal{B}_{m,n}^r} \lambda^{|\tau_{\Lambda_n}|} \sum_{\substack{\eta \in \mathcal{B}_{m,n}^r \\ \phi(\eta) = \tau}} \lambda^{|\eta_{\Lambda_n}| - |\tau_{\Lambda_n}|}}{\sum_{\eta \in \mathcal{A}_{m,n}^r} \lambda^{|\eta_{\Lambda_n}|}} \leq \frac{1}{3}, \quad (8) \end{aligned}$$

which establishes Eq. (5). To construct the mapping ϕ , we begin by defining a contour elimination operation. Define an *island* in γ_\bullet as the interior of a non-contractible primitive closed path¹ formed by the faces of γ . The hexagons of the island that share an edge with faces of γ are of the same color. We call this set of hexagons the “boundary wall” and we say that the island is blue (red, green) if its boundary wall is blue (resp., red or green). Note that there can be further contours contained in the island (as shown in Fig. 4a); however, the shifts that we discuss below apply to the entire island, including possibly those contours.

Contour elimination operation $\psi : \mathcal{X}(\mathbb{A}) \times \Gamma \mapsto \mathcal{X}(\mathbb{A})$. Let $\gamma \in \Gamma(\omega)$ be a contour of some configuration $\omega \in \mathcal{X}(\mathbb{A})$. Define the operation $\psi(\omega, \gamma)$ as follows.

1) Shift the islands:

- If γ is red, shift all blue islands by one unit in the northwest (NW) direction (i.e., add $\mathbf{b}_2 - \mathbf{b}_1$ to each site) and shift all green islands by one unit in the northeast (NE) direction.
- If γ is green, shift all blue islands NE by one unit and shift all red islands NW by one unit.
- If γ is blue, shift all red islands one unit NE and all

¹*Non-contractible* means non-null-homotopic, and *primitive* means that it is not a composition of two nontrivial cycles.

green islands one unit NW.

This operation shifts the islands of the two colors other than the color of γ in the directions that ensure that the shifted sites do not compete for the same spot (if they did, then before the shift, the sites of these two colors would be adjacent). Denote the set of shifted sites by $T(\gamma_\bullet)$.

- 2) Change the color of the shifted sites to agree with the color of the contour γ . In Fig. 4b, the colors of the (lightly filled) green and red hexagons change to blue and green, respectively.
- 3) Add new occupied sites to the shifted configuration such that the resulting configuration is in $\mathcal{X}(\mathbb{A})$. These vertices will have the color of γ , thus erasing the contour. The newly added hexagons are shown in light blue in Fig. 4b.

Note that the directions of the shift are not unique; we only need to make sure that collisions do not arise as a result.

Lemma 3.3. *The operation $\psi(\cdot, \gamma)$ is injective and for every n such that $\gamma \subset \Lambda_n$, we have*

$$|\psi(\omega, \gamma)_{\Lambda_n}| - |\omega_{\Lambda_n}| = \frac{|\gamma|}{6}, \quad (9)$$

where $|\gamma|$ is the number of faces contained in γ .

Proof: Let $\eta = \psi(\omega, \gamma)$. To argue that ψ is injective given γ , we simply note that one can reconstruct ω from η and γ . Knowing γ , we also know the boundary of the contour. To reconstruct ω , we first remove the hexagons added in Step 3. They are identifiable because they cannot be a part of $T(\gamma_\bullet)$ because of the direction of the shift. Next, we identify $T(\gamma_\bullet)$ and undo the shift, recovering ω .

To show Eq. (9), we first observe that the vertices added in Step 3 are contained in $\tilde{\gamma} := (\gamma \cup \gamma_\bullet) \setminus T(\gamma_\bullet)$. Indeed, the shift operation only moves vertices (filled hexagons) in γ_\bullet , and one cannot occupy any extra vertex (or put an extra filled hexagon) in γ_\circ or $T(\gamma_\bullet)$. Note that all faces outside $\tilde{\gamma}$ that are adjacent to $\tilde{\gamma}$ have the same color after the shift; thus, the only way to make $\psi(\omega, \gamma)$ maximal is to cover all faces in $\tilde{\gamma}$ by adding vertices (hexagons) of the same color. In addition, the shift operation does not change the number of covered faces, so to cover every empty face in $\tilde{\gamma}$, we need $|\gamma|/6$ hexagons. ■

We now proceed to establish (7). Since $\eta \in \mathcal{B}_{m,n}^r$ is m -green, there exists a red contour that separates the green homogeneous region containing Λ_m^W and the red boundary. Let γ be that contour and define $\phi(\omega) := \psi(\omega, \gamma)$. By (9) we have

$$\sum_{\substack{\eta \in \mathcal{B}_{m,n}^r: \\ \phi(\eta) = \tau}} \lambda^{|\eta_{\Lambda_n}| - |\tau_{\Lambda_n}|} = \sum_{\substack{\eta \in \mathcal{B}_{m,n}^r: \\ \phi(\eta) = \tau}} \lambda^{-\frac{|\gamma(\eta)|}{6}} \leq \sum_{\substack{\gamma \in \Gamma: \\ \Lambda_m^W \subset \gamma_\bullet}} \lambda^{-\frac{|\gamma|}{6}}, \quad (10)$$

where the inequality follows since we are able to reconstruct η given $\gamma \in \Gamma$ and τ . Now let Γ_l^m be the collection of all contours of size l (with l faces) that contain Λ_m^W . We have

$$\sum_{\gamma \in \Gamma: \Lambda_m^W \subset \gamma_\bullet} \lambda^{-\frac{|\gamma|}{6}} = \sum_{l \geq 4m} \frac{|\Gamma_l^m|}{\lambda^{l/6}}. \quad (11)$$

Lemma 3.4. $|\Gamma_l^m| = O(l^2 15^l)$

Proof: A subgraph is associated with any contour, as in Fig. 2b, and distinct contours give rise to distinct subgraphs. We will estimate the number of subgraphs of G_{Λ_n} with degrees between 2 and 4 (of course, not all of them give rise to valid contours). Fix a vertex $v \in V(G_{\Lambda_n})$ to be the starting point of the contour γ . Since γ surrounds the origin, there are at most $O(l^2)$ possible locations for v .

Further, there are at most $\binom{6}{2} + \binom{6}{3} + \binom{6}{4} = 50$ ways to choose the neighbors of v . From each of the neighbors, we can choose a further set of neighbors in at most $\binom{5}{1} + \binom{5}{2} + \binom{5}{3} = 25$ ways. Carrying on recursively, this gives an upper bound of $50 \times 25^{l-2} = O(25^l)$ for the number of connected l -vertex subgraphs of G_{Λ_n} starting with v . Accounting for the $O(l^2)$ possible choices of v , this gives us a (crude) upper bound of $O(l^2 25^l)$ for the number of possible contours in Γ_l^m .

To reduce the base from 25 to 15, we count the subgraphs more carefully. The options for choosing the neighbors in a construction step other than the first one are shown in Fig. 8. We start with a vertex, w , shown by a black-filled face. It is connected to (at least) one face (vertex) in the graph, u , shown as a dash-filled triangle. u and w can be edge- or vertex-adjacent, and we examine both options as indicated in the captions, choosing the larger count for the overall estimate. The face w can have degree 4, 3, or 2, depending on the contour, so we have to choose 3, 2, or 1 additional neighbors, shown as lightly filled faces. For instance, Figs. 8a and 8b address the case of 3 neighbors in addition to u . Both figures list all the $\binom{5}{3} = 10$ possible choices; however, not all of them can be realized in the graph: patterns can be disallowed because they either force an empty hexagon (e.g., patterns 5-10 in Fig. 8a) or they cannot appear in the contour (e.g., patterns 8, 9 in Fig. 8d). The number of realizable patterns is 5 for degree 4 (Fig. 8a), 7 for degree 3 (Fig. 8c or Fig. 8d), and 3 for degree 2 (Fig. 8f), yielding 15 as an upper bound. ■

Thus, if $\lambda > 15^6$, the series in (11) converges, and its sum can be made smaller than $\frac{1}{3}$ by choosing m large enough. The proof of (6) proceeds analogously by interchanging the roles of red and green, resulting in $\mu_n^g(\mathcal{R}_m | \mathcal{G}_m \cup \mathcal{R}_m) \leq \frac{1}{3}$.

We note that it may be possible to reduce the exponent base even further if we account for the properties of the graph G_{Λ_n} , summarized as follows.

Lemma 3.5. *The graph G_{Λ_n} is bipartite, planar, 2-connected, with degrees between 2 and 4.*

Proof: 2-connectedness is obvious, and the statement about the degrees was proved above. To show that G_{Λ_n} is bipartite, note that faces pointing up can connect only to faces pointing down (cf. Fig. 8).

Let us prove that the subgraph of G_{Λ_n} whose vertex set forms a contour, γ , admits a planar embedding in \mathbb{R}^2 . Denote this subgraph by G_γ ; see Fig. 2. Place each vertex in the geometric center of the face to which it corresponds and connect the adjacent vertices with straight-line segments. Let U, V be two faces in γ and let u, v be the corresponding vertices of G_γ . Vertices u and v are adjacent in G_γ if the

faces U and V are edge- or vertex-adjacent. If they are edge-connected, then the edge uv cannot intersect other edges of G_γ : the only edges of G_γ that can be present are incident to u or v and do not intersect uv . Now suppose that U and V are vertex-connected. The edge uv can intersect another edge of G_γ only if there is another vertex-connected pair of faces, U' and V' , that shares the vertex of \mathbb{A} common to U and V . However, such empty pairs U, V and U', V' cannot appear in the contour together because this would force an empty hexagon. ■

While there are results on the growth rate of the number of 2-connected planar graphs [31], the estimates for the count of the graphs they give do not improve on our estimate. The same is true for other known results on the count of planar graphs of various kinds [32]–[34].

4. PHASE COEXISTENCE: THE LOW-ACTIVITY REGIME

At low activity, Gibbs distributions are determined by the ground states of the model. One naturally expects that for sufficiently small λ , typical configurations are local perturbations of these ground states. A useful tool for formalizing this idea is provided by the Pirogov-Sinai theory [12, Ch. 7], [35]. This theory asserts precisely that when λ is sufficiently small, all extremal Gibbs measures arise as thermodynamic limits of finite-volume Gibbs measures with boundary conditions given by (stable) periodic ground states (PGSs). Moreover, configurations sampled from these extremal measures typically differ from the corresponding ground state only by local perturbations.

A configuration $\omega \in \mathcal{X}(\mathbb{A})$ is called periodic if there exists $v \in \mathbb{A}$ such that $\omega_i = \omega_{i+v}$ for all $i \in \mathbb{A}$. As before, we represent vertices in \mathbb{A} using their coordinates in the basis $(\mathbf{b}_1, \mathbf{b}_2)$.

The main result in this part is stated next.

Theorem 4.1. *Let $\lambda < 1$. There are 14 PGSs for the maximal hard-core model on \mathbb{A} . For sufficiently small λ , each ground state η gives rise to an extremal periodic Gibbs measure, μ_η , and all such measures are generated by the PGSs. The measures μ_η for different PGSs are mutually singular. For $\lambda \rightarrow 0$ and any η , the measure μ_η converges weakly to δ_η .*

The proof begins with identifying the PGSs. Let \mathcal{X}^{per} be the set of periodic configurations in $\mathcal{X}(\mathbb{A})$. For $\omega \in \mathcal{X}^{\text{per}}$, define the density of ω as follows:

$$\delta(\omega) := \lim_{n \rightarrow \infty} \frac{|\omega_{\Lambda_n}|}{|\Lambda_n|},$$

where $|\omega_{\Lambda_n}|$ denotes the number of occupied sites in $\Lambda_n \in \mathbb{A}$, see Def. 1.1 (the limit clearly exists). The following quantity is called the *energy density*:

$$e(\omega) := \lim_{n \rightarrow \infty} \frac{1}{|\Lambda_n|} \mathcal{H}_{\Lambda_n}(\omega) = -(\ln \lambda) \delta(\omega),$$

where $\mathcal{H}_\Lambda(\omega) = -|\omega_\Lambda| \ln \lambda$ is the Hamiltonian.

It is known [12, Lemma 7.4] that $\eta \in \mathcal{X}(\mathbb{A})^{\text{per}}$ is a PGS if and only if its energy density is minimal:

$$e(\eta) = \inf_{\omega \in \mathcal{X}(\mathbb{A})^{\text{per}}} e(\omega).$$

Depending on whether $\lambda > 1$ or not, $e(\omega)$ is minimized by maximizing or minimizing $\delta(\omega)$. In other words, PGSs are equivalently defined as the sparsest (low activity) and densest (high activity) configurations in $\mathcal{X}(\mathbb{A})^{\text{per}}$.

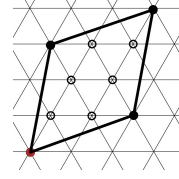


Fig. 6: Sparse PGSs for $\mathcal{X}(\mathbb{A})$ of density $1/7$.

Theorem 4.2. *The density of PGSs of $\mathcal{X}(\mathbb{A})$ satisfies $\frac{1}{7} \leq \delta(\omega) \leq \frac{1}{3}$. There are exactly 3 periodic configurations with density $\frac{1}{3}$ and 14 periodic configurations with density $\frac{1}{7}$.*

Proof: Bounds on the density are proved by constructing tilings of the plane with Voronoi regions of the occupied vertices and counting the proportion of covered vertices. Let $\omega \in \mathcal{X}(\mathbb{A})^{\text{per}}$ be a periodic configuration, defined by the condition $\omega_i = \omega_{i+v}$ for all $i \in \mathbb{A}$ and some $v = (v_1, v_2) \in \mathbb{A}$. This means that there is a parallelogram tile with sides $v_1 \mathbf{b}_1, v_2 \mathbf{b}_2$ whose shifts fill the plane, and then

$$\delta(\omega) = \frac{|\omega_{v_1 \times v_2}|}{v_1 v_2},$$

where (by abuse of notation) $\omega_{v_1 \times v_2}$ denotes ω restricted to the parallelogram. The first step is to use periodicity to identify this tile with the torus $\mathbb{T}_{v_1, v_2} = \{(i, j) \mid i \in \mathbb{Z} \pmod{v_1}, j \in \mathbb{Z} \pmod{v_2}\}$, so that every 0 in $\omega_{v_1 \times v_2}$ is adjacent to at least one 1. Next let us count the number, N , of pairs (u, v) in which u and v are adjacent sites in \mathbb{T}_{v_1, v_2} , with the property that $\omega_u = 1$ and $\omega_v = 0$. Since every occupied site $u \in \text{supp}(\omega_{v_1 \times v_2})$ is adjacent to six unoccupied sites, we have $N = 6|\omega_{v_1 \times v_2}|$. On the other hand, every unoccupied site v in the torus \mathbb{T}_{v_1, v_2} is adjacent to at least one and at most three occupied sites; so we also have $v_1 v_2 - |\omega_{v_1 \times v_2}| \leq N \leq 3(v_1 v_2 - |\omega_{v_1 \times v_2}|)$. Substituting N , we obtain

$$v_1 v_2 - |\omega_{v_1 \times v_2}| \leq 6|\omega_{v_1 \times v_2}| \leq 3(v_1 v_2 - |\omega_{v_1 \times v_2}|),$$

which implies that $\frac{1}{7} \leq \delta(\omega) \leq \frac{1}{3}$. Moreover, we have $\delta(\omega) = \frac{1}{7}$ iff equality holds in the left inequality above, i.e., every unoccupied site v in the torus \mathbb{T}_{v_1, v_2} is adjacent to exactly one occupied site. Similarly, we have $\delta(\omega) = \frac{1}{3}$ iff equality holds in the right inequality, i.e., every unoccupied site v in the torus \mathbb{T}_{v_1, v_2} is adjacent to exactly three occupied sites.

The maximal-density PGSs for \mathbb{A} are the three configurations with all the same-color vertices occupied. To identify the lowest-density PGSs, we note that periodicity implies the existence of a tiling of the (discrete) plane. Indeed, \mathbb{A} can be tiled with parallelograms, Fig. 7, which also shows a PGS for \mathbb{A} . Six other PGSs are obtained as shifts of the one containing the origin, shown as the red-colored site in Fig. 6 (the 6 unfilled sites correspond to the shifts). Together with the mirror images, the maximal hard-core model has 14 sparse PGSs. ■

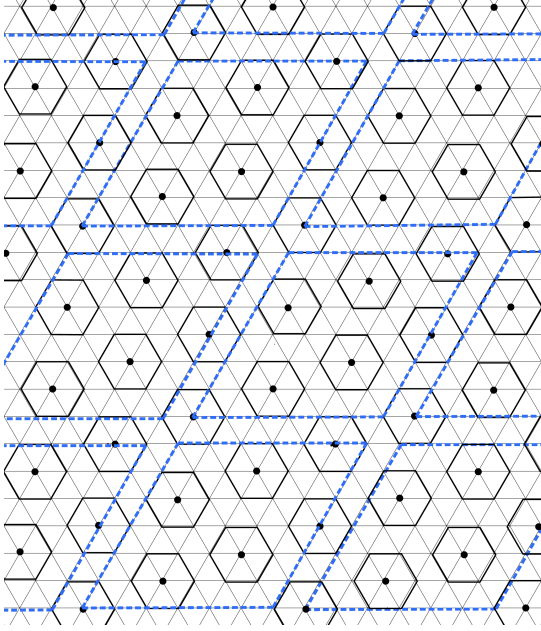


Fig. 7: A sparse PGS: each unoccupied vertex is adjacent to *exactly one* occupied vertex. The figure shows one of the 14 PGSs for \mathbb{A} of density $1/7$. The 7×7 parallelograms form a tiling of \mathbb{R}^2 .

The main part of the proof of Theorem 4.1 is devoted to verifying a Peierls-type condition [35, Sec.1.5]. Loosely speaking, this condition controls the increase of energy caused by a perturbation of a ground state, and is satisfied if this increase is proportional to the size of the perturbation. This condition can be rigorously expressed using the contour formalism.

Let \mathcal{Q} be the set of all 7×7 patterns that occur in $\mathcal{X}(\mathbb{A})$ and let us partition \mathbb{A} into disjoint 7×7 blocks. Namely, let

$$\mathcal{P}_0 := \{(x, y) \in \mathbb{A} : 0 \leq x < 7, 0 \leq y < 7\}$$

be the block with the lower left corner at the origin (recall that we are using the basis $\mathbf{b}_1, \mathbf{b}_2$). We may then reinterpret configurations in $\mathcal{X}(\mathbb{A})$ using a block-spin representation: consider a partition of \mathbb{A} into blocks of the form $\mathcal{Q}(l, m) := \mathcal{P}_0 + 7(l, m)$, where $(l, m) \in \mathbb{A}$, and encode each block with an element of \mathcal{Q} . See Fig. 7; note that $\mathcal{Q}(l, m)$ is the 7×7 box with the bottom left corner at $(7l, 7m)$.

Let \mathcal{G} denote the set of 14 periodic ground states for $\lambda < 1$ and let $\mathcal{Q}_p \subset \mathcal{Q}$ be the set of 7×7 patterns arising from the periodic ground states. Then, in this block-spin representation, each ground state corresponds to a constant configuration $Q^{\mathbb{A}}$ for some $Q \in \mathcal{Q}_p$.

Let $\omega \in \mathcal{X}(\mathbb{A})$ and $\bar{\omega}$ be the corresponding block-spin representation. Denote by $\bar{\omega}_{l,m}$ the restriction of ω to $\mathcal{Q}(l, m)$.

Definition 4.1 (Correct and incorrect blocks).

(i) Let $Q \in \mathcal{Q}_p$. The block $\mathcal{Q}(l, m)$ is called *Q-correct* in ω if $\bar{\omega}_{l+i, m+j} = Q$ for all $i, j \in \{0, \pm 1\}$. In other words, a correct block at (l, m) matches the pattern Q together with all of its 8 neighboring blocks. We call a block *incorrect* if it is not *Q-correct* for any $Q \in \mathcal{Q}_p$.

(ii) An incorrect block is said to be *t-defective* if it intersects

at least one defective triangle (even on a single vertex). An incorrect block is called *n-defective* if it is not *t-defective*: these blocks are neighbors of a *t-defective* block, which themselves take values from \mathcal{Q}_p . The neighboring blocks of $\mathcal{Q}(l, m)$ are $\mathcal{Q}(l \pm 1, m \pm 1)$.

We define a *contour* in ω as a maximal connected component γ formed of incorrect blocks². The energy associated with a contour γ is determined by the number of occupied vertices that γ encloses. The Hamiltonian restricted to γ is

$$\mathcal{H}_\gamma(\omega) = -|\omega_\gamma| \ln \lambda.$$

Let η be one of the periodic ground states. The relative Hamiltonian of ω with respect to η , restricted to γ , is given by $\mathcal{H}_\gamma(\omega | \eta) = (|\eta_\gamma| - |\omega_\gamma|) \ln \lambda$. Below, we will assume that η is a local perturbation of ω , i.e., they differ in a finite number of sites. By definition of the ground state, $\mathcal{H}_\gamma(\omega | \eta) \geq 0$. The Peierls condition, moreover, requires that

$$\mathcal{H}_\gamma(\omega | \eta) \geq \rho |\gamma|$$

for some constant $\rho > 0$. Using the expression for \mathcal{H} and recalling that $\lambda < 1$, we can write this explicitly as

$$|\omega_\gamma| - |\eta_\gamma| \geq \alpha |\gamma|, \quad (12)$$

where $\alpha := -\frac{\rho}{\ln \lambda} > 0$.

Remark 1. There is a technical issue concerning the way of verifying the Peierls condition. Often γ is defined as the “thick” boundary of all the incorrect blocks within $\mathcal{Q}(l, m)$, i.e., the union of all contours in the region, see e.g., [12, Ch.7]. Another possibility appearing in the literature ([35, Sec.1.5], [21]) is verifying condition (12) for individual contours, and then aggregating these inequalities for the final result. We will follow the second option without further mention. \triangleleft

One approach to analyzing the number of occupied vertices in a configuration $\omega \in \mathcal{X}(\mathbb{A})$ is through the *Delaunay triangulation* defined by its support. Let $\omega \in \mathcal{X}(\mathbb{A})$. To every occupied site, i , there corresponds a polygon formed of the points of \mathbb{R}^2 that are closer to i than to any other occupied site of ω . The collection of these polygons forms a Voronoi partition of \mathbb{R}^2 defined by ω . The Delaunay triangulation defined by ω is a triangulation of \mathbb{R}^2 constructed as the dual graph of the Voronoi partition defined by ω ; namely, the circumcenters of the triangles are the vertices of the Voronoi diagram. The vertices of the triangles are the sites of \mathbb{A} . Importantly, Delaunay triangulations have the following characterization: the circumcircles of the triangles do not contain any occupied sites of ω other than the vertices of their triangles.

Call a triangle with vertices at the lattice points *regular* if it is equilateral of side length $\sqrt{7}$ and call it *defective* otherwise. If ω is one of the periodic ground states, then every Delaunay triangle is regular. Call a triangle with vertices $u, v, w \in \mathbb{A}$ *feasible* if (1) it does not contain a lattice point that is not adjacent to an occupied site in any ω whose support includes u, v, w ; (3) none of the pairs in u, v, w are neighbors \mathbb{A} . Delaunay triangles are clearly feasible.

²Here we abuse the notation: this notion of a contour is different from the one introduced in Definition 3.1.

The following statement is proved by examining all possible triangles in a Delaunay triangulation of a MIS.

Lemma 4.3. *For $\omega \in \mathcal{X}(\mathbb{A})$, the area of any defective triangle in a Delaunay triangulation defined by ω is at most $\frac{3\sqrt{3}}{2}$.*

Proof: Below, we do not distinguish ω from its support. We first claim that any circle in \mathbb{R}^2 of radius $\rho = \sqrt{7/3} \approx 1.527$ contains a point in ω . Let C be a such circle and suppose that $C \cap \omega = \emptyset$ (C contains no occupied vertices of ω). The center of this circle may not lie in \mathbb{A} but is at distance $\leq \sqrt{3}/3$ from one of the lattice points. This point is either in ω or at distance 1 from a point in ω , so there is an occupied vertex, v , no further than ρ from the center of the circle.

We will examine all the feasible triangles with circumradius $\leq \rho$ with vertices in ω . It suffices to examine triangles with one vertex at $(0, 0)$ since if there is a MIS with a triangle of some shape elsewhere, its shift is also a MIS. Therefore, all the triangles will be assumed to have one of their vertices at the origin. The remaining two vertices are contained in the circle of radius ρ with center at the origin, including possibly its circumference. There are 36 such vertices in \mathbb{A} not counting the origin. Examining all the possible triangles (with the help of computer) proves the lemma. ■

Let $\omega \in \Omega$ and let $\mathbb{T}_k := \mathbb{T}_{k,k}$ be a $7k \times 7k$ torus in \mathbb{A} as defined in the proof of Theorem 4.2. Denote by $\mathcal{T}_\omega(\mathbb{T}_k)$ a Delaunay triangulation of \mathbb{T}_k defined by ω .

Lemma 4.4. *For any $\omega \in \Omega$,*

- (a) *the triangles in $\mathcal{T}_\omega(\mathbb{T}_k)$ form a tessellation of \mathbb{T}_k ;*
- (b) *the number of triangles $|\mathcal{T}_\omega(\mathbb{T}_k)| = 2|\omega_{\mathbb{T}_k}|$.*

Proof: The first part follows by definition. The second claim is justified as follows. Place a disk of area $\pi/8$ around each occupied site; since the distance between the sites is at least 1, the disks do not overlap. Each triangle intersects exactly three such disks—one for each of its vertices. Moreover, since the sum of the interior angles is π , the sum of the areas of the three sectors cut out by the triangle is $1/2$. Rephrasing, the area within the disks covered by each triangle is exactly $1/2$. On the other hand, every disk is fully covered by the triangles, so the count of triangles is twice the number of disks, which is also the number of occupied sites. ■

The specific version of (12) that we establish appears next.

Theorem 4.5. *Let $\omega \in \mathcal{X}_0$, let η be a periodic ground state, and let γ be the contour formed of incorrect blocks. Then*

$$|\omega_\gamma| - |\eta_\gamma| \geq \max\left(1, \frac{1}{378}|\gamma|\right).$$

Proof: Observe that the blocks in the immediate neighborhood of γ are Q -correct for some values of $Q \in \mathcal{Q}_p$. Recall that the Q -constant block-spin configuration is a periodic ground state. Therefore, ω_γ can be extended using Q -tiles, which gives us a configuration τ on \mathbb{T}_k for a sufficiently large k . In other words, we define a configuration τ on \mathbb{T}_k such that $\tau_\gamma = \omega_\gamma$ and $\tau_{\gamma^c} = \eta'_{\gamma^c}$ for some other periodic ground state

of our model³. Importantly, $|\tau_{\gamma^c}| = |\eta_{\gamma^c}|$, where $\gamma^c = \mathbb{T}_k \setminus \gamma$.

By Lemma 4.3, any defective triangle has area at most $\frac{3\sqrt{3}}{2}$. If we replace one or more regular triangles (which have area $\frac{7\sqrt{3}}{4}$) with defective (smaller) ones, then to tile \mathbb{T}_k we will use more triangles than the number of triangles in $\mathcal{T}_\eta(\mathbb{T}_k)$ (this number equals $\frac{|\mathbb{T}_k|}{7\sqrt{3}/4} = 2k^2/7$, where $|\cdot|$ denotes the area). The total number of triangles in a triangulation is even (it is twice the number of occupied sites), so the total count of triangles increases by at least 2, and the number of occupied sites increases by at least 1.

The size of $\mathcal{T}_\tau(\mathbb{T}_k)$ can be estimated as follows. Denote by R a generic triangle and let $N_0(\tau)$ and $N_d(\tau)$ be the number of regular and defective triangles in $\mathcal{T}_\tau(\mathbb{T}_k)$, respectively. We have

$$\begin{aligned} |\mathbb{T}_k| &= \sum_{\text{defective } R} |R| + \frac{7\sqrt{3}}{4}N_0(\tau) \\ &\leq \frac{3\sqrt{3}}{2}N_d(\tau) + \frac{7\sqrt{3}}{4}N_0(\tau) \end{aligned}$$

using the fact that the area of a defective triangle is at most $\frac{3\sqrt{3}}{2}$, proved in Lemma 4.3. Re-arranging this inequality, we obtain

$$N_0(\tau) + N_d(\tau) \geq \frac{|\mathbb{T}_k|}{7\sqrt{3}/4} + \frac{1}{7}N_d(\tau).$$

Thus, the triangulation \mathcal{T}_τ increases the count of triangles over \mathcal{T}_η , namely,

$$|\mathcal{T}_\tau(\mathbb{T}_k)| \geq |\mathcal{T}_\eta(\mathbb{T}_k)| + \frac{1}{7}N_d(\tau).$$

Since each t -defective incorrect block is surrounded by at most 8 n -defective incorrect blocks (Fig. 7), all of which enter γ , and each defective triangle intersects at most 3 incorrect blocks, we obtain

$$3N_d(\tau) \geq \#\{\text{t-defective blocks}\} \geq \frac{|\gamma|}{9}.$$

Note that $\omega_\gamma = \tau_\gamma$ (since the only changes are outside γ) and $|\omega_{\gamma^c}| \geq |\tau_{\gamma^c}|$ (since ω_{γ^c} may span defective triangles, and τ_{γ^c} gives rise only to regular ones). We continue as follows:

$$\begin{aligned} |\omega_{\mathbb{T}_k}| &= |\omega_\gamma| + |\omega_{\gamma^c}| \geq |\tau_\gamma| + |\tau_{\gamma^c}| \\ &= \frac{1}{2}|\mathcal{T}_\tau(\mathbb{T}_k)| \geq \frac{1}{2}\left(|\mathcal{T}_\eta(\mathbb{T}_k)| + \frac{N_d(\tau)}{7}\right) \\ &\geq \frac{1}{2}\left(|\mathcal{T}_\eta(\mathbb{T}_k)| + \frac{|\gamma|}{189}\right) \\ &= |\eta_{\mathbb{T}_k}| + \frac{|\gamma|}{378}. \end{aligned}$$

Since we argued earlier that $|\omega_{\mathbb{T}_k}| \geq |\eta_{\mathbb{T}_k}| + 1$, the proof is complete. ■

The first claim of Theorem 4.1 was proved in Theorem 4.2 above; thus, in the maximal hard-core case at low activity, periodic ground states form a single equivalence class defined by lattice symmetries (shifts and reflections). The remaining

³If γ is not simply connected, it may happen that ω_{γ^c} agrees with different periodic ground states in different connected components of \mathbb{T}_k defined by γ . This will not matter for the argument below, since we rely on the number of occupied sites rather than on the ground states themselves.

parts of the proof amount to collecting the relevant results from the literature devoted to the Pirogov-Sinai theory, among which we single out [35], [36], as well as Ch. 7 of [12]. Details of the application of this theory for the (standard) hard-core case appear in [9, Theorem III], which also gives specific references to the literature required to complete the proof. Here we limit ourselves to a brief summary.

It is known that every extremal Gibbs measure μ_η is generated by a periodic ground state, η , namely,

$$\mu_\eta = \lim_{\Lambda \uparrow \mathbb{Z}^2} \mu_\Lambda(\cdot | \eta),$$

where the limit is in the van Hove sense. This follows from [36] and the main result of [37]. Generally, there may exist periodic ground states that do not give rise to (extremal) Gibbs measures; however, there is at least one state, η , that does [36]. Moreover, all ground states η' obtained from η by translations and reflections on \mathbb{A} also give rise to Gibbs measures $\mu_{\eta'}$. The remaining claims also follow immediately from [36].

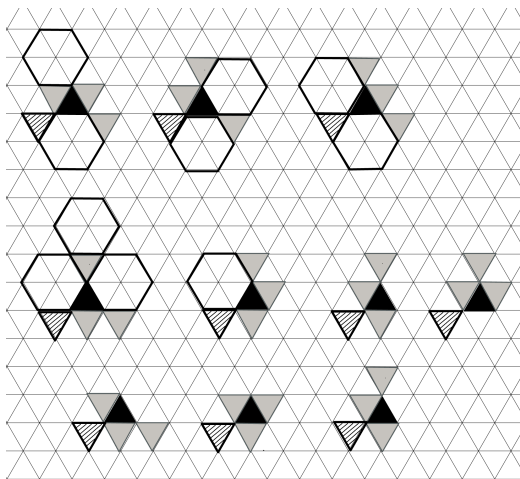
Remark 2. A natural counterpart of the triangular lattice \mathbb{A} is given by its dual, the honeycomb lattice \mathbb{H} . The maximal hard-core model is easily defined, and one can address the same set of questions as studied for \mathbb{Z}^2 and \mathbb{A} . The low-activity case can be analyzed with little difficulty relying on the same set of ideas. In particular, the least-populated PGSSs of the maximal hard-core model on \mathbb{H} have density 1/4 since every occupied vertex has exactly 3 unoccupied neighbors, and every unoccupied vertex is connected to exactly one occupied. At the same time, the high-activity case is less obvious because the contour-erasing approach used here encounters difficulties (construction of the mapping ϕ used to erase the contours is not obvious).

ACKNOWLEDGMENT: The first two authors were partially supported by NSF grants CCF2330909 and CCF2526035.

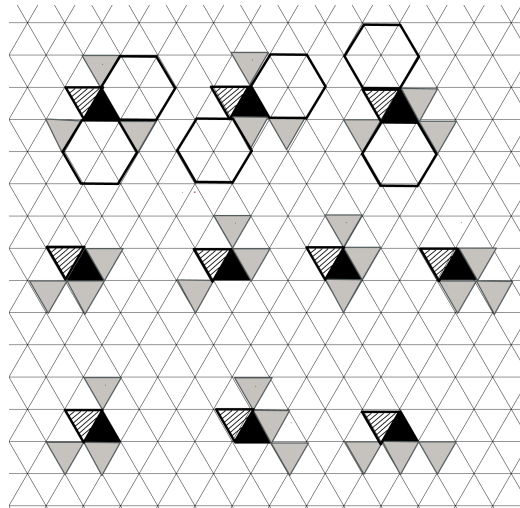
REFERENCES

- [1] V. Ramkumar, S. Balaji, B. Sasidharan, M. Vajha, M. N. Krishnan, and P. V. Kumar, “Codes for distributed storage,” *Foundations and Trends in Communications and Information Theory*, vol. 19, pp. 547–813, 2022.
- [2] O. Elishco and A. Barg, “Recoverable systems,” *IEEE Trans. Inform. Theory*, vol. 68, no. 6, pp. 3681–3699, Jun. 2022.
- [3] G. Wang, A. Barg, and N. Kashyap, “Recoverable systems as interaction models: A study by example,” in *2025 IEEE International Symposium on Information Theory (ISIT)*. IEEE, 2025, pp. 1–6.
- [4] —, “The maximal hard-core model as a recoverable system: Gibbs measures and phase coexistence,” *arXiv preprint arXiv:2510.19746*, 2025.
- [5] D. Weitz, “Counting independent sets up to the tree threshold,” in *STOC’06: Proceedings of the 38th Annual ACM Symposium on Theory of Computing*. ACM, New York, 2006, pp. 140–149.
- [6] R. Restrepo, J. Shin, P. Tetali, E. Vigoda, and L. Yang, “Improved mixing condition on the grid for counting and sampling independent sets,” *Probab. Theory Related Fields*, vol. 156, no. 1-2, pp. 75–99, 2013.
- [7] A. Blanca, Y. Chen, D. Galvin, D. Randall, and P. Tetali, “Phase coexistence for the hard-core model on \mathbb{Z}^2 ,” *Combin. Probab. Comput.*, vol. 28, no. 1, pp. 1–22, 2019.
- [8] R. J. Baxter, “Hard hexagons: exact solution,” *J. Phys. A*, vol. 13, no. 3, pp. L61–L70, 1980.
- [9] A. Mazel, I. Stuhl, and Y. Suhov, “High-density hard-core model on triangular and hexagonal lattices,” *Annales Henri Poincaré*, vol. 26, pp. 3321–3381, 2025.
- [10] T. R. Albrecht, H. Arora, V. Ayanoor-Vitikkate, J.-M. Beaujour, D. Bédau, D. Berman, A. L. Bogdanov, Y.-A. Chapuis, J. Cushen, E. E. Dobisz *et al.*, “Bit-patterned magnetic recording: Theory, media fabrication, and recording performance,” *IEEE Transactions on Magnetics*, vol. 51, no. 5, pp. 1–42, 2015.
- [11] F. Tejo, D. Toneto, S. Oyarzún, J. Hermosilla, C. S. Danna, J. L. Palma, R. B. da Silva, L. S. Dorneles, and J. C. Denardin, “Stabilization of magnetic skyrmions on arrays of self-assembled hexagonal nanodomains for magnetic recording applications,” *ACS Applied Materials & Interfaces*, vol. 12, no. 47, pp. 53454–53461, 2020.
- [12] S. Friedli and Y. Velenik, *Statistical Mechanics of Lattice Systems: A Concrete Mathematical Introduction*. Cambridge University Press, Cambridge, 2018.
- [13] B. Simon, *Phase Transitions in the Theory of Lattice Gases*. Cambridge University Press, 2025.
- [14] E. Zehavi and J. K. Wolf, “On runlength codes,” *IEEE Transactions on Information Theory*, vol. 34, no. 1, pp. 45–54, 1988.
- [15] G. Han and B. Marcus, “Asymptotics of input-constrained binary symmetric channel capacity,” *The Annals of Applied Probability*, vol. 19, no. 3, pp. 1063–1091, 2009.
- [16] G. Sabato and M. Molkaiaie, “Generalized belief propagation for the noiseless capacity and information rates of run-length limited constraints,” *IEEE Transactions on Communications*, vol. 60, no. 3, pp. 669–675, 2012.
- [17] M. Molkaiaie and H.-A. Loeliger, “Monte Carlo algorithms for the partition function and information rates of two-dimensional channels,” *IEEE Transactions on Information Theory*, vol. 59, no. 1, pp. 495–503, 2013.
- [18] O. Sabag, H. H. Permuter, and N. Kashyap, “The feedback capacity of the binary erasure channel with a no-consecutive-ones input constraint,” *IEEE Transactions on Information Theory*, vol. 62, no. 1, pp. 8–22, 2016.
- [19] Y. Li and G. Han, “Asymptotics of input-constrained erasure channel capacity,” *IEEE Transactions on Information Theory*, vol. 64, no. 1, pp. 148–162, 2018.
- [20] O. Sabag, H. H. Permuter, and N. Kashyap, “Feedback capacity and coding for the BIBO channel with a no-repeated-ones input constraint,” *IEEE Transactions on Information Theory*, vol. 64, no. 7, pp. 4940–4961, 2018.
- [21] A. Mazel, I. Stuhl, and Y. Suhov, “High-density hard-core model on \mathbb{Z}^2 and norm equations in ring $\mathbb{Z}[\sqrt[6]{-1}]$,” *arXiv preprint arXiv:1909.11648*, 2019.
- [22] L. Dall’Asta, P. Pin, and A. Ramezani, “Statistical mechanics of maximal independent sets,” *Physical Review E*, vol. 80, no. 6, p. 061136, Dec. 2009.
- [23] R. Burton and J. E. Steif, “Non-uniqueness of measures of maximal entropy for subshifts of finite type,” *Ergodic Theory Dynam. Systems*, vol. 14, no. 2, pp. 213–235, 1994.
- [24] A. Katok and B. Hasselblatt, *Introduction to the modern theory of dynamical systems*. Cambridge University Press, 1999.
- [25] O. Häggström, “On phase transitions for subshifts of finite type,” *Israel Journal of Mathematics*, vol. 94, no. 1, pp. 319–352, 1996.
- [26] S. Forchhammer and J. Justesen, “Bounds on the capacity of constrained two-dimensional codes,” *IEEE Trans. Inform. Theory*, vol. 46, no. 7, pp. 2659–2666, 2000.
- [27] R. M. Roth, P. H. Siegel, and J. K. Wolf, “Efficient coding schemes for the hard-square model,” *IEEE Transactions on Information Theory*, vol. 47, no. 3, pp. 1166–1176, 2002.
- [28] A. Sharov and R. M. Roth, “Two-dimensional constrained coding based on tiling,” *IEEE transactions on information theory*, vol. 56, no. 4, pp. 1800–1807, 2010.
- [29] R. L. Dobrushin, “The problem of uniqueness of a Gibbsian random field and the problem of phase transitions,” *Functional analysis and its applications*, vol. 2, no. 4, pp. 302–312, 1968.
- [30] S. Greenberg and D. Randall, “Slow mixing of Markov chains using fault lines and fat contours,” *Algorithmica*, vol. 58, no. 4, pp. 911–927, 2010.
- [31] E. A. Bender, Z. Gao, and N. C. Wormald, “The number of labeled 2-connected planar graphs,” *The Electronic Journal of Combinatorics*, pp. R43–R43, 2002.
- [32] O. Giménez and M. Noy, “Asymptotic enumeration and limit laws of planar graphs,” *Journal of the American Mathematical Society*, vol. 22, no. 2, pp. 309–329, 2009.
- [33] M. Noy, V. Ravelomananana, and J. Rué, “Enumeration of labelled 4-regular planar graphs ii: Asymptotics,” *Journal of Combinatorial Theory, Series B*, vol. 154, pp. 273–316, 2022.

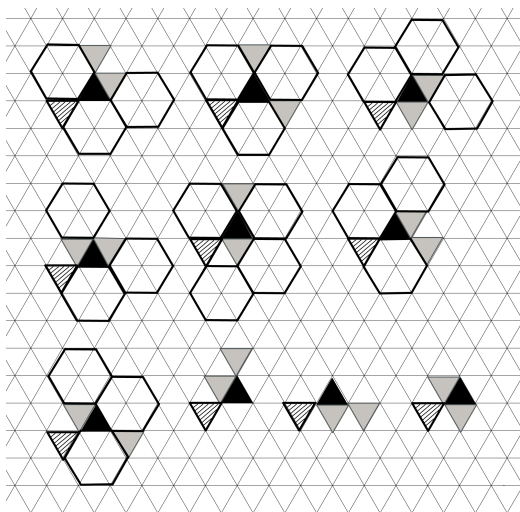
- [34] M. Bodirsky, M. Kang, M. Löffler, and C. McDiarmid, “Cubic graphs and related triangulations on orientable surfaces,” *The Electronic Journal of Combinatorics*, vol. 25, no. 1, p. P1.30, 2018, arXiv preprint 1612.01358 (2016).
- [35] M. Zahradník, “A short course on the Pirogov-Sinai theory,” *Rendiconti di Matematica, Serie VII*, vol. 18, pp. 411–486, 1998.
- [36] —, “An alternate version of Pirogov-Sinai theory,” *Commun. Math. Phys.*, vol. 93, pp. 559–581, 1984.
- [37] R. Dobrushin and S. Shlosman, “The problem of translation invariance of Gibbs states at low temperatures,” *Sov. Sci. Rev. C Math. Phys.*, vol. 5, pp. 53–196, 1985.



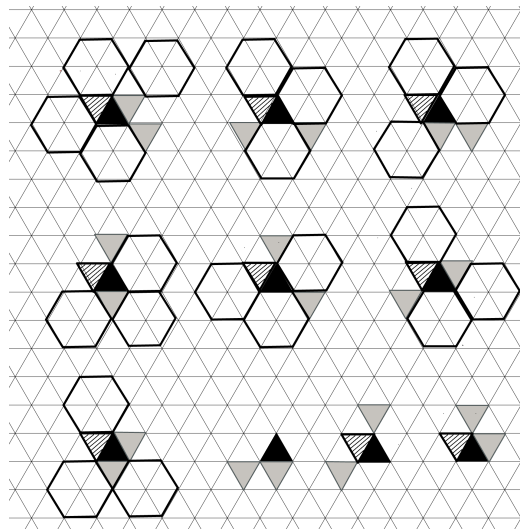
(a) 4 neighbors, vertex-connected



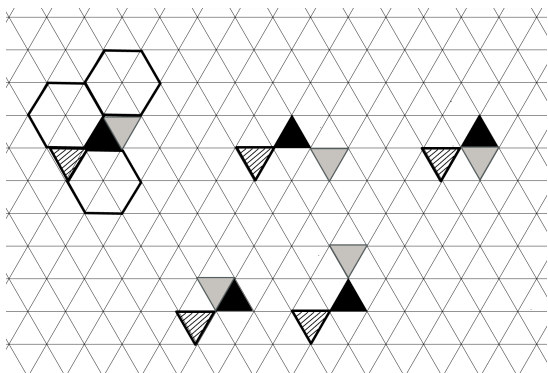
(b) 4 neighbors, edge-connected



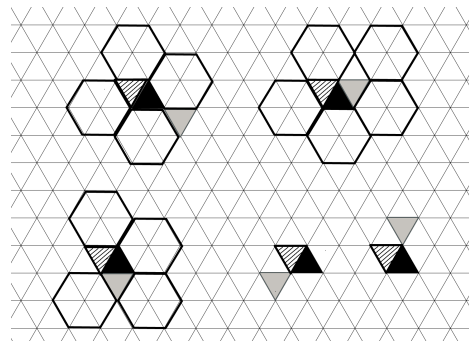
(c) 3 neighbors, vertex-connected



(d) 3 neighbors, edge-connected



(e) 2 neighbors, vertex-connected



(f) 2 neighbors, edge-connected

Fig. 8: A single step of contour construction in the proof of Theorem 3.4. Suppose that the black-filled face is adjacent to the dash-filled face and both are a part of the contour. We are estimating the number of ways the contour can continue from the black face. Figs. 8a and 8b address the case of three neighbors not counting the dash-filled one, and Figs. 8c and 8d and Figs. 8e and 8f do the same for two and one neighbor, respectively. The potential neighbors are shown as lightly filled faces. Patterns that can arise in the graph are shown as parts of the configuration, with hexagons for occupied vertices. Further explanations appear in the proof of the lemma.